JMEPEG (2011) 20:932–940
DOI: 10.1007/s11665-010-9735-9

1059-9495/$19.00

Enhanced Erosion Protection of TWAS Coated Ti6Al4V Alloy Using Boride Bond Coat and Subsequent Laser Treatment

B.S. Mann, Vivek Arya, and B.K. Pant

(Submitted April 17, 2010; in revised form June 8, 2010)

The material commonly used in low-pressure high-rating super critical/ultra super critical steam turbines as well as guide and moving blades of high speed aero compressors is Ti6Al4V alloy. These blades are severely affected owing to erosion which leads to drop in efficiency and increase in maintenance cost. This article deals with SHS 7170 coating on Ti6Al4V alloy using twin wire arc spraying (TWAS), enhancing its bonding by providing a thin bond coat and then treating with high-power diode laser (HPDL). Significant improvement in erosion resistance of this multilayer coating has been achieved because of the formation of fine-grained micro structure due to rapid heating and cooling rates associated with the laser surface treatment. After laser surface treatment, the fracture toughness of this multilayer has improved manifold. The water droplet and particulate erosion test results along with the damage mechanism are reported and discussed in this article.

Keywords diode laser, solid particulate erosion, steam turbine, Ti6Al4V alloy, twin wire arc, water droplet erosion

1. Introduction

The water droplet erosion (WDE) and solid particle erosion (SPE) of steam path surfaces in steam turbines have been a major concern. SPE is believed to arise due to formation of magnetite, an oxide of iron on the inside of steam generator ferritic alloy boiler header, drum, and tubes. During the initial hours of operation (around 80,000 h), little or no erosion is observed; however, after an additional 40,000 h of operation, severe erosion occurs. In fact, the leading edges of inlet buckets of a typical 800-MW steam turbine have eroded 12-13 mm from their original dimensions in this time increment (Ref 1-3). This is because a magnetite (brittle oxide) layer builds up to a certain point and then cracks/spalls usually due to temperature transient during start up or during major load change. This magnetite scale breaks up into hard angular particles which pass through the turbine and erode the components. Significant erosion has been experienced on the diaphragm, inlet of guide, and moving blades, and this becomes more critical on the areas where water droplet (due to condensation of steam) exists especially in high-rating critical and supercritical steam turbines above 500 MW, likely futuristic ultra-supercritical up to 1310 MW, and also in nuclear steam turbine of all ratings. The combined effects of water droplets and solid particles erode the steam path components quickly.

B.S. Mann, Vivek Arya, and **B.K. Pant**, Surface Coatings and Treatment Laboratory, BHEL, Corporate R&D Division, Vikasnagar, Hyderabad 500093, India. Contact e-mail: balbir@bhelrnd.co.in.

On the other hand, the guide and moving blades of a compressor used in aero engines are made of titanium alloys. Titanium alloys are favored because of their light weight, high strength to weight ratio, high corrosion resistance, and good high-cycle fatigue properties. The erosion damage occurring due to foreign objects directly hitting the blades during take off and landing is very severe, and the repair of such damages becomes expensive especially for commercial airlines. The loss in power due to reduced surge margins of compressor blades is a big concern. It is also a serious problem for military aircraft and turbine-powered armored vehicles that operate in severe dust-laden environments. Helicopter engines are susceptible to large amounts of dust and sand ingestion during takeoff, hover, and landing. The erosion due to rain and ice with water droplets near sonic speeds puts additional demand on the durability of compressor vanes, blades, and helicopter rotor blades. In case of helicopter rotor blades, the size and characteristic impact velocity of the particulate flow are several times larger than those of rotating components of an aero compressor.

There are mainly two types of coating systems which are generally used to combat WDE and SPE. These are (a) diffusion coating i.e., plasma ion nitrocarburizing/boronizing and TiN/TiC coating by cathodic arc deposition (CAD) or by large area filtered arc deposition (LAFAD) technique and (b) thermally sprayed coatings i.e., by detonation gun, by high velocity oxy-fuel or by twin wire arc spraying (TWAS) (Ref 4-15). Hard TiN/TiC coatings by CAD, LAFAD technique, or plasma ion nitrocarburizing/boronizing have size limitations whereas the thermally sprayed coatings and laser treatment do not have such limitations. For alloy steels, WDE-related studies have already been carried out, and these are reported in Ref 7. However, for titanium alloy, water droplet and particulate erosion-related studies require further investigations.

For a 1310-MW ultra-supercritical steam turbine, Mitubishi Heavy Industries Ltd has optimized on 74-in. titanium alloy blades for their last stage. GE-Toshiba is working on optimizing

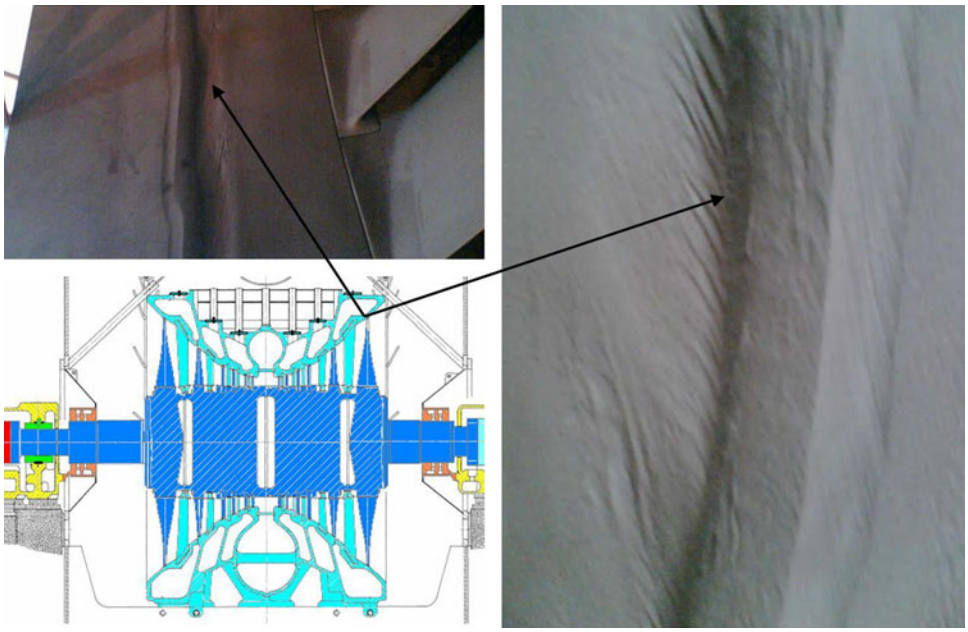

Fig. 1 After an operation of 1,15,000 h, the inner wall casing thickness of a typical 225-MW steam turbine is reduced to 18 mm from its original value of 40 mm due to water droplet erosion

hybrid titanium and steel alloy guide blades (Ref 16, 17). Due to their large size and high rpm, the erosion of these blades is a challenging problem. The edges of conventional LPST steel blades are protected either by induction or flame hardening at 980 ± 5 °C or by fixing stellite plates from the blade tip toward the root of the blade by brazing (Ref 18, 19). These plates, for a 200-MW turbine, are generally 320 mm long, 12 mm wide, and 1.50 mm thick and are made from stellite 6 alloy having a hardness of 421 HV_{10}. However, stellite cannot be brazed on Ti6Al4V alloy. Among the various hard thermal spray coatings, twin wire arc using cored wires is gaining interest for application of erosion and corrosion due to their high spray rate, reduced set-up time, higher deposit efficiency (60-70% as against 30-35% for HP-HVOF coating), and reduced coating cost (20-30% cheaper as compared to HVOF coating). Recently, Nano Steel has reported an achievement of nano scale coating by TWAS process that compares well with HVOF coatings. This new development with SHS 7170-cored wire was enabled by extensive alloy design studies which revealed specific combination of atom ratios that readily form metallic glass structures at cooling rates in the range of 10^4 to 10^5 K/s while using TWAS (Ref 10-11). The "as-sprayed" coatings contain a high fraction of two dimensional defect phase boundaries. To eliminate these defects, these coatings are recommended to be heat treated above 700 °C. During second heat treatment above 700 °C, these glass precursors readily transform into nano-scale composite structure and give bond strength more than 450 kg/cm^2; micro hardness values more than 1000 HV_{300}, and they have excellent wear and corrosion resistance (Ref 8, 10, 11). It has been reported that carbide $(Fe\text{-}Cr\text{-}W\text{-}Mo)_{23}C_6$- and boride $(Fe\text{-}Cr\text{-}Mo\text{-}W)_3B$-type nano hard phases of 66% volume fraction are formed, which are responsible for the improved performance. In fact, with increased thickness, these values exceed the bond strength, and failure in the form of detachment takes place. After post-spray heat treatment, these materials cause the devitrification of the metallic glass contents and this results in very low residual stresses, excellent wear resistance, and better impact properties (Ref 8). Twin wire arc cored wire coatings treated with HPDL are effective in tackling such erosion problems for big components and are economical because of high outage cost of high value components. Figure 1 shows the erosion damage that has occurred (approximately 150 mm wide) on a cast steel casing periphery around the LPST blade tips of a 225-MW steam turbine after an operation of 1,15,000 h. The casing is 40 mm deep and is made of two halves weighing 36.4 tons (upper) and 41.5 tons (lower). Due to the on-going erosion, the wall thickness of the casing in some areas has been reduced down to 18 mm from its original thickness of 40 mm.

To combat combined effect of particulate and droplet erosion, TWAS SHS 7170 coating was applied on Ti6Al4V alloy. By providing a thin boride layer in between SHS 7170 coating and Ti6Al4V alloy and treating with HPDL, a dramatic improvement in bonding of TWAS SHS 7170 coating to Ti6Al4V alloy has occurred. The coating is designated as TWAS SHS $7170^{Plus\ B}$. The mechanism behind the improved bonding of this coating after laser treatment, its WDE, and SPE results are reported and discussed in this article.

2. Experimental Procedure

2.1 Twin Wire Arc Spraying

Using Hobart Tafa 9000 (TWAS 9000) system, the SHS 7170 cored wire (1.6-mm diameter) was sprayed on Ti6Al4V round ($\varnothing$ 12.7 × 40 mm) and flat samples (50 × 50 × 6 mm). While performing the TWA spraying, the manipulation of the samples was done by six plus two axis robot, and spraying parameters, such as arc voltage, current, spray distance, rotation, and transverse speed were optimized. The samples were grit blasted using 24-mesh alumina grit at an air pressure of 5-5.5 kg/cm^2 (g). The spraying parameters adopted were as

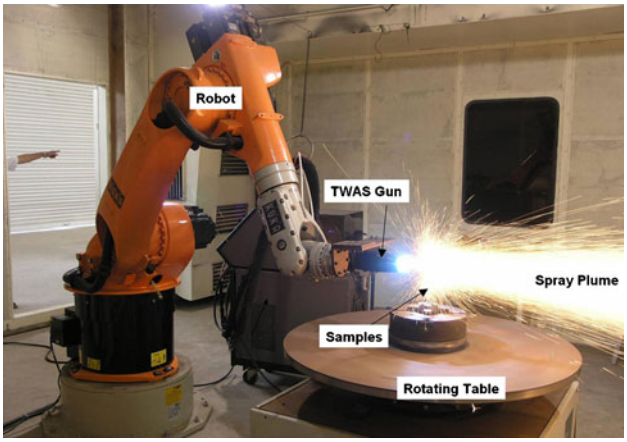

Fig. 2 The complete set up for performing TWAS coating

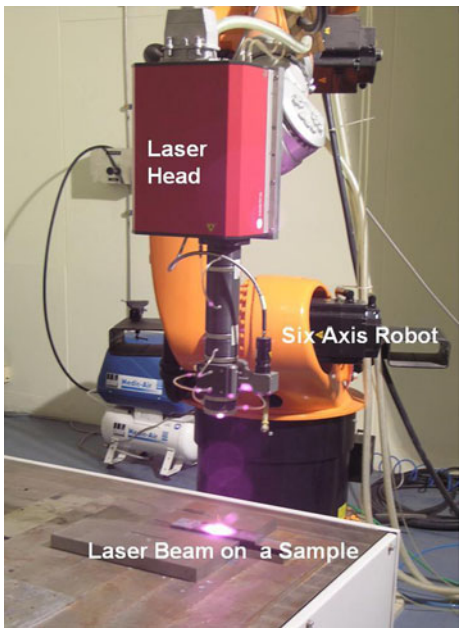

Fig. 3 The complete set up for performing HPDL treatment

Table 1 Spray parameters of TWAS 9000 as per technical manual and Ref 7

Equipment type	Hobart Tafa, TWAS 9000
Primary air pressure	5.44 kg/cm^2 (g)
Nozzle cap/positioner	Green/Long C
Arc voltage	33 V
Arc current	200 A
Round and flat sample sizes	∅ 12.7 × 40 mm and 50 × 50 × 6 mm
Spray angle	90°

per Ref 7. Figures 2 and 3 show the complete setup for carrying out TWAS coating and HPDL treatment. Table 1 gives the TWAS details and parameters. A thin boride layer of thickness 70-100 μm is provided in between Ti6Al4V alloy and TWAS SHS 7170 coating, which has overcome the thermal mismatch and resulted in excellent diffusion between Ti6Al4V alloy and the coating. The TWAS SHS 7170 coating thickness was in the range of 300-350 μm.

2.2 HDPL Surface Treatment

Droplet erosion samples of diameter 12.7 mm × 40 mm length having internal threading M8 were made of Ti6Al4V alloy. HPDL surface treatment was carried out on each round sample using 4.6-kW diode laser with the laser head mounted on a six plus two axis robot. Details of the experimental test set up are given in Ref 7, 20. Optics of 20 mm × 2.8 mm was used. Laser beam power was controlled in a closed loop by a two color pyrometer and a uniform surface temperature of 1525-1575 °C was maintained, and the TWAS coating gets remelted and metallurgically modified (changes in porosity, fracture toughness, and hardness). The complete system was controlled by the robot controller. The robot was programmed in such a way that the laser beam tracked the round as well as flat samples at a controlled speed ranging from 2 to 5 mm/s ensuring that both melting and diffusion of the coating are completed in single pass. A fixture was fabricated to hold and rotate the samples while carrying out HPDL surface treatment. Each round sample was fixed in a self-centered three-jaw chuck at one end and supported by a fixture on the other end. The fixture has a rotating seal, so that the samples can rotate freely and air used for cooling the samples does not leak. Rapid cooling of the sample was carried out during HPDL surface treatment by introducing compressed air having volumetric flow rate of 15-16 m^3/h through the M8-tapped hole. This air is capable of removing the heat at a rate of 160-180 W which is comparable to the heat removed in a bulk material during laser surface treatment. Before start of the experiment, the samples were thoroughly cleaned using acetone to make sure that the surfaces are free from dust, oil etc. The laser power densities used for TWAS-coated round samples were in the range of 1840-2015 W/(cm^2/s) whereas, for the TWAS-coated flat disc samples, these were in the range of 2300-2350 W/(cm^2/s). It was observed that there was complete melting of the coating. For the comparative purpose, uncoated Ti6Al4V rounds samples were also laser treated in the higher temperature range of 1625-1675 °C with the above optics. It was observed that at these laser power densities and scan speeds, there was no melting of Ti6Al4V alloy. The laser-treated samples were stress relieved before characterizing and testing. Laser treatment of materials is a very versatile technique and used for other applications as well (Ref 21, 22).

2.3 Testing and Characterization

The Vicker's micro hardness of HPDL-treated and untreated samples was measured using Tukon 2100 Macro/Micro hardness tester by applying a load of 300 g with a dwell time of 13 s. Seven measurements of hardness at different locations were taken per sample, and average of the results has been reported in the article. The fracture toughness (k_{1c}) of the surface coating plays a significant role in the erosion resistance, and it was evaluated by the surface indentation technique using the same Tukon 2100 hardness tester (Ref 14). Loads up to 30 kg were applied on the coatings, and the indent's diagonal (a) and crack length (c) were measured. Using Cu Kα radiation and nickel filter, x-ray diffraction was also taken.

2.4 Particulate Erosion Testing

Particulate erosion tests were carried out using high pressure water jet impingement erosion test facility. It consists of a convergent nozzle through which a fixed amount of mineral

sand flows and mixes well with the water in a mixing block. The slurry passes through a tungsten carbide throat of diameter 4 mm × 40 mm long, providing a uniform jet velocity of 29.0 m/s. Rectangular samples of size 50 × 50 × 6 mm can be kept in front of a sand-laden water jet at various angles ranging from 0° to 90°, and the sand-laden water is passed in a controlled manner. These samples were ground finished to obtain a surface roughness below 0.1 μm. The flow parameters such as water flow rate, pressure (up stream of the tungsten nozzle), and sand flow rate were monitored. The jet velocities were determined by volume flow rate divided by the area of the carbide nozzle. Typical water jet pressure readings were in the range of 12-12.5 kg/cm^2 (g) for obtaining jet velocities in the range of 29-30 m/s. The schematic diagram of the slurry erosion test facility is given in Ref 23. The slurry erosion resistance of all the samples was determined by mass loss measurement. The samples were weighed before and after the erosion test to an accuracy of ±0.10 mg using a precision balance. The following test conditions were maintained.

Erodent type	Mineral sand of hardness 1100 HV
Erodent size and concentration	180-250 μm and 7500 ppm
Water velocity and impingement angle	29 m/s and 45°
Specimen size and test duration	50 × 50 × 6 mm and 10 min

At the end of the test, the samples were removed and ultrasonically cleaned with acetone to remove any slurry or debris. Each test was repeated to determine the experimental reliability and error. The experimental error was within ±3%.

2.5 Droplet Erosion Testing of HPDL Surface-Treated Samples

The details of droplet erosion test facility which has been designed and fabricated as per ASTM G-73-98, are given in Ref 20. In short, the test facility consists of a 700-mm diameter chamber and a round stainless steel disc where the test samples are positioned. Samples, 40 mm in length and 12.7 mm in diameter are affixed on the periphery of the disc. The disc is rotated at 79.166 cycles/s to obtain the test sample tangential velocity of 147.0 m/s. Two water jets impinge on the cylindrical test samples and cause impingement erosion. As such, a relative velocity of 147.6 m/s is obtained. The mass of water impacted from these jets per cycle is 0.035 mL equivalent to energy flux values of 57.167×10^6 J/m^2 s, and experimental values of test parameters are given in Table 2.

Table 2 Experimental test conditions

Conditions	Test parameters
Volume of water impacted per cycle	0.035 mL
Water impact energy (1/2 mV^2)	0.380 J
Water energy flux, J/m^2 s	57.167×10^6
Water mass flux	4.0 m/s
Relative water velocity	147.6 m/s
Test sample size	∅ 12.70 × 40 mm
Number of specimens used	12
Test duration cycles	3.84×10^6
Angle of impact	0-90°
Impact frequency	79.166 cycles/s
Experimental accuracy	±15.5%

The WDE tests were carried out up to 3.84×10^6 cycles and discontinued afterward due to excessive damage occurring on the Ti6Al4V alloy sample. The water droplet impact energy (1/2 mV^2) used in this study is approximately twice that actually occurring on 74-in. moving blade of 1310-MW ultra supercritical steam turbine for 800-μm water droplets (0.15 J).

The test duration depending on energy and mass fluxes was selected in such a way as to achieve steady-state erosion in short duration. The accuracy and repeatability of the tests have been established on the base material which is taken as a reference material. The extent of erosion damage is calculated as cumulative volume loss (cumulative mass loss divided by the material density). The results have been plotted in the form of cumulative volume loss versus number of cycles. The salt concentrations in the water were as observed: Calcium Hardness ~134, Magnesium Hardness ~166, M-Alkalinity ~206, P-Alkalinity ~nil, Chlorides ~97, Sulphates ~47, and Total Solids ~690 having pH 7.93 and conductivity 0.894 millimhos/cm. This has resulted in slightly lower volume loss in WDE as compared to those reported earlier in Ref 24. Laser-treated X10CrNiMoV1222 steel samples were also studied for the comparison.

2.6 Deflection Measurements and Fatigue Testing

For deflection measurements, round discs of 91.20 mm diameter and 6 mm thickness were used. The round discs were chosen because the tips of the steam turbine/compressor blades have a curvature, though their radii may be different. The HPDL parameters, such as the temperature of the sample, HPDL power, and laser scan speed were monitored and maintained similar to those of cylindrical samples used for droplet erosion testing. The deflections in round discs were measured using a 3D coordinate measurement machine. The fatigue test samples were fabricated from these laser-treated discs, and the fatigue tests were performed at 400 and 550 MPa using Schenk make reverse bending machine.

3. Results and Discussion

3.1 Micro Hardness and Fracture Toughness

The TWAS SHS 7170 coating without boride layer after laser treatment developed cracks which became visible during grinding. This is due to thermal mismatch between Ti6Al4V alloy and TWAS SHS 7170 coating. The micro hardness of TWAS SHS 7170$^{\text{Plus B}}$ coating after laser treatment varies from 654 to 987 HV_{300}. (Lower values on the boride layer and higher values on the laser-treated top layer.) A thin boride bond coat in between Ti6Al4V alloy and SHS 7170 has helped to overcome this thermal mismatch, and no cracks appeared during grinding. The fracture toughness (k_{1c}) measurement of the composite coating was carried out in a similar way as reported in Ref 14. The k_{1c} values calculated by the Evans-Charles formula and for "as-sprayed" TWAS SHS 7170 coating was 3.70 MPa $\sqrt{m}$ at a load of 10 kg (average of 3 readings). The laser-treated "TWAS SHS 7170$^{\text{Plus B}}$ coating" has not developed any cracks even at 30-kg load, and hence, k_{1c} could not be measured. Figures 4 and 5 shows the indentation on the cross section of the coatings. This confirms that a significant improvement in fracture toughness has occurred due to bond coat and HPDL treatment. This is one of the main reasons of its improved erosion resistance.

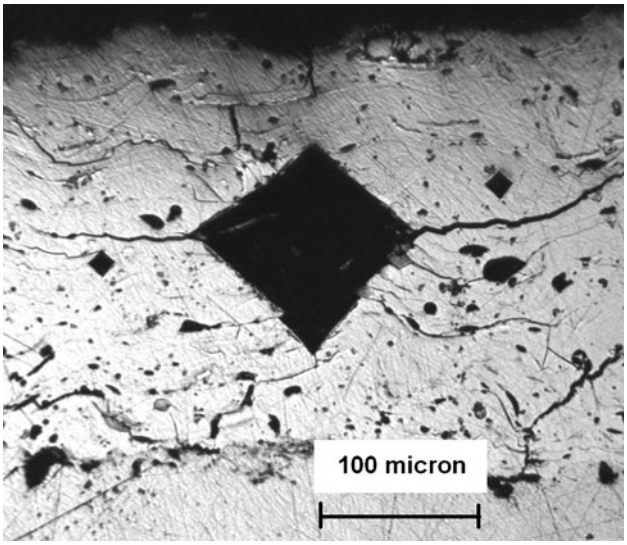

Fig. 4 Optical micrograph of "as-coated" TWAS SHS 7170 coating

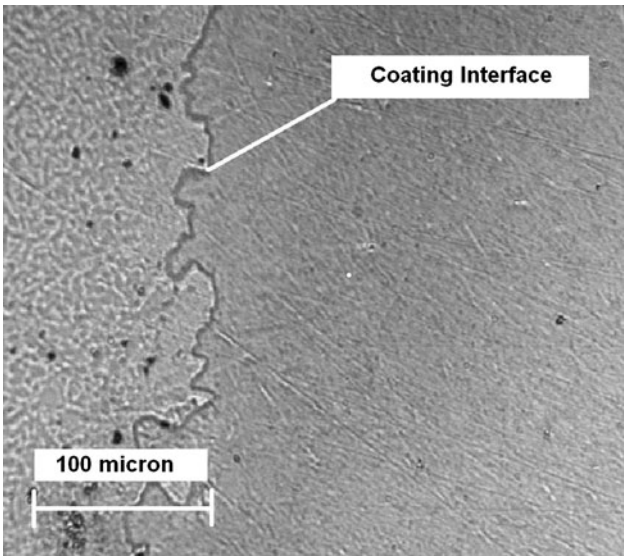

Fig. 5 Optical micrograph of laser-treated TWAS SHS $7170^{Plus\ B}$ coating (interfaces are well diffused)

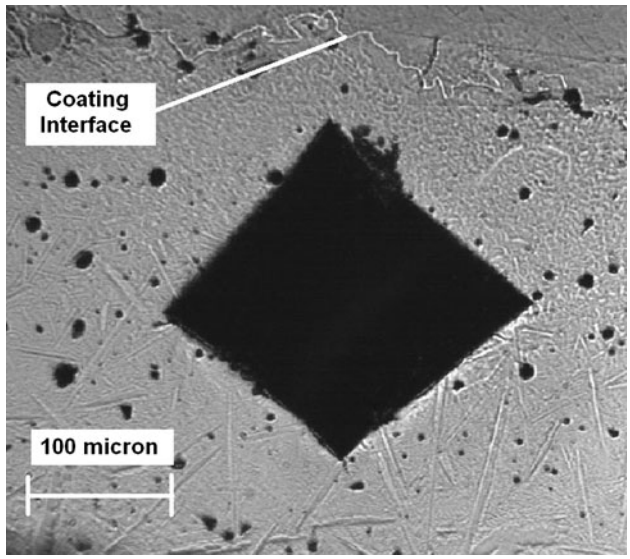

Fig. 6 Optical micrograph of laser-treated TWAS SHS $7170^{Plus\ B}$ coating (sharp needles in the laser-treated area)

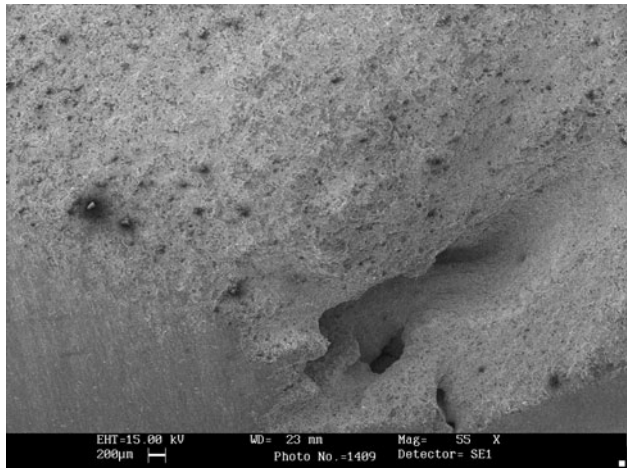

Fig. 7 SEM of titanium alloy at 55× magnification after WDE testing of 3.84 million cycles (extensive damage)

The coating Interface is shown in Fig. 5 and 6. These figures confirm the integrity of the coating.

3.2 Scanning Electron Micrographs and X-Ray Diffraction Test Results

The scanning electron micrographs (SEMs) of water droplet-eroded samples are shown in Fig. 7-13. In case of laser-treated samples (both coated and uncoated), the material removal phenomena appears to be grain by grain (refer Fig. 10, 12) whereas, in the case of untreated Ti6Al4V alloy sample, it appears to be layer by layer (refer Fig. 8). The SEM of laser-treated Ti6Al4V alloy sample shows relatively larger grain size as compared to that of laser-treated TWAS SHS $7170^{Plus\ B}$ coating. The fast heating and cooling rates associated with laser treatment has resulted in finer microstructures of the TWAS SHS $7170^{Plus\ B}$ coating as compared to laser-treated Ti6Al4V alloy sample (due to better thermal diffusivity of coating) and, hence, further enhanced its droplet erosion resistance. The microstructure of laser-treated TWAS SHS $7170^{Plus\ B}$ coating is free from pores, voids, as well as inter boundary defects, and shows the presence of fine carbide $(Fe\text{-}Cr\text{-}W\text{-}Mo)_{23}C_6$- and boride $(Fe\text{-}Cr\text{-}Mo\text{-}W)_3B$-type nano hard phases (needles).

The x-ray diffraction of HPDL surface-treated and untreated samples were carried out by using Philips X-pert system (Philips, Netherlands). XRD analysis confirms the presence of iron, and chromium along with major unknown amorphous phases, and these are already reported earlier in Ref 7.

3.3 Particulate Erosion Test Results

The particulate erosion resistance of laser-treated TWAS SHS $7170^{Plus\ B}$ coating has improved approximately two times as compared to "as-sprayed" coating. Volume loss of "as-sprayed" TWAS SHS 7170 and that of laser-treated TWAS

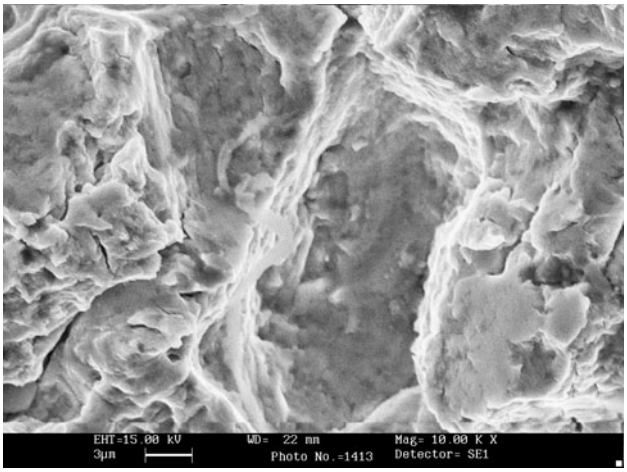

Fig. 8 SEM of titanium alloy at 10,000× magnification after WDE testing of 3.84 million cycles (material removal layer by layer)

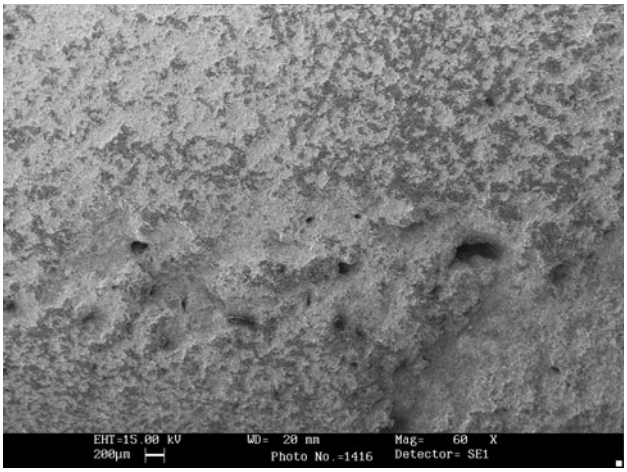

Fig. 9 SEM of laser-treated titanium alloy at 60× magnification after WDE testing of 3.84 million cycles (less damage)

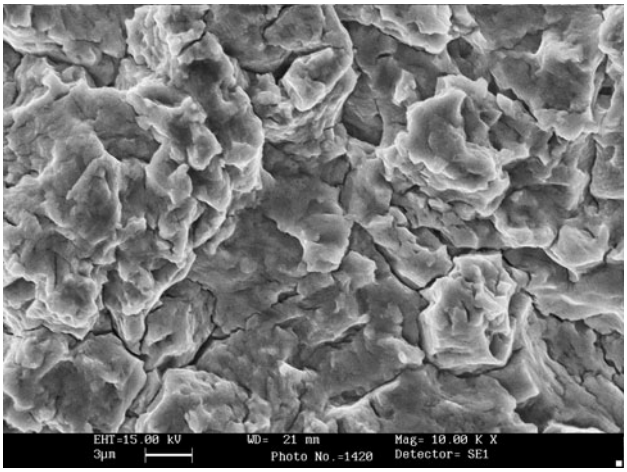

Fig. 10 SEM of laser-treated titanium alloy at 10,000× magnification after WDE testing of 3.84 million cycles (grain size approximately 4-5 µm)

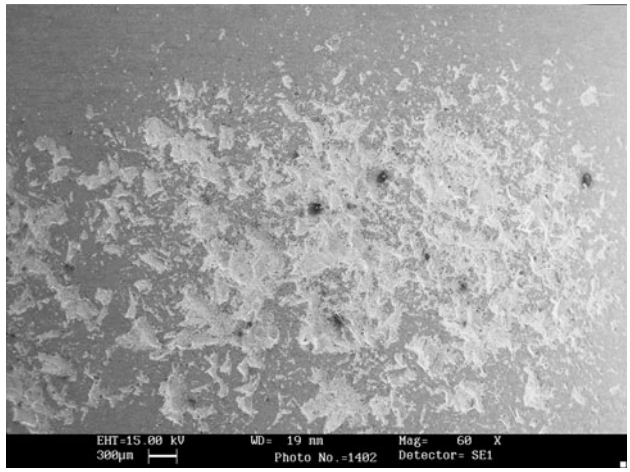

Fig. 11 SEM of laser-treated TWAS SHS 7170$^{\text{Plus B}}$ coating at 60× magnification after WDE testing of 3.84 million cycles (damage nil)

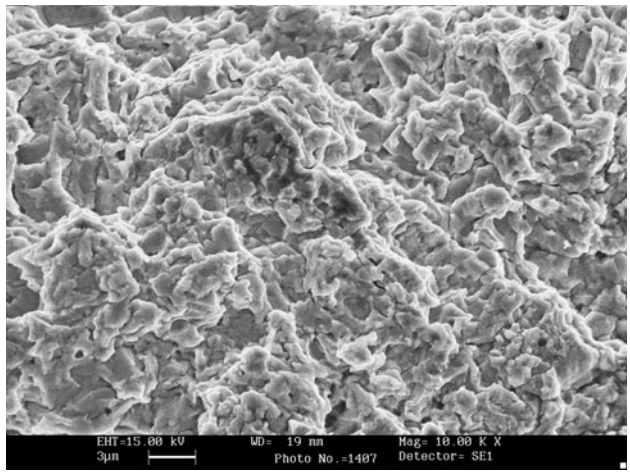

Fig. 12 SEM of laser-treated TWAS SHS 7170$^{\text{Plus B}}$ coating at 10,000× magnification after WDE testing of 3.84 million cycles (grain size approximately 2-3 µm)

SHS 7170$^{\text{Plus B}}$ coating are given in Fig. 14. The laser-treated TWAS SHS 7170$^{\text{Plus B}}$ coating, as explained earlier, is dense, and free from voids and pores (refer Fig. 6). This is the main reason for its improved performance. The particulate erosion resistance of laser-treated Ti6Al4V alloy has also improved by ∼28%.

3.4 Droplet Erosion Test Results

The droplet erosion test results of laser-treated TWAS SHS 7170$^{\text{Plus B}}$ coated sample along with laser-treated Ti6Al4V and X10CrNiMoV1222 alloy samples are shown in Fig. 15. It is seen from the figure that, at a water droplet energy flux level of 57.167×10^6 J/m^2 s, the laser-treated TWAS SHS 7170$^{\text{Plus B}}$ coated sample is much superior to laser-treated X10CrNiMoV1222 steel and laser-treated Ti6Al4V alloy samples. The incubation period for this coating has also got prolonged. The excellent WDE resistance of TWAS SHS 7170$^{\text{Plus B}}$ coating after HPDL surface treatment is due to finer grain morphology

which is achieved by higher cooling rates due to forceful extraction of heat from the sample using compressed air and by providing larger inner cooling surface area of the round sample as shown in inset of Fig. 15 (threaded area). The coating upper layer is free from micro cracks, pores, void, oxides etc., and the coating is having excellent inter-diffusion bonding. The "as-sprayed" TWAS SHS 7170 coating has peeled off during initial droplet erosion testing (~47500 cycles). This is because "as-sprayed" TWAS coatings have voids, pores, inter-boundary defects as inherent defects which are visible in micrograph shown in Fig. 4.

3.5 Deflection and Fatigue Test Results

Maximum permanent bending of the order of 540 μm in laser-treated Ti6Al4V and 740 μm in the laser-treated TWAS SHS 7170$^{Plus\ B}$-coated disc samples was observed. Deflections in the laser scan direction (X axis) for both types of the disc samples were less than those that occurred across the laser scan direction (Y axis). The radii of curvature arising due to deflections are given in Fig. 16. It is seen from Fig. 16 that the curvature is concave in both the directions and their magnitudes are different. This has resulted in compressive residual stresses in X and Y directions, and their magnitudes depend on their deflections which are permanent in nature. The deflections and hence the stresses developed in a particular material depend upon the geometry of the sample, its thermal response, HPDL power, its scan speed, and direction. For the blades, the value of these stresses may be different, but their trends of being compressive along and across the laser beam remain unchanged. For laser-treated TWAS SHS 7170$^{Plus\ B}$-coated sample, the deflections in both directions is more than the laser-treated uncoated sample, which indicates that the stresses are more than that occurred for laser-treated uncoated sample. Using the two-point reverse bending fatigue test set-up, Ti6Al4V AS (as-received), Ti6Al4V LH (laser-treated). and TWAS SHS 7170$^{Plus\ B}$ (laser-treated) samples were tested for fatigue failure. The results are given below in Table 3.

From the above data, it is clear that laser treatment of Ti6Al4V does not affect the fatigue property whereas for the laser-treated TWAS SHS 7170$^{Plus\ B}$ Ti6Al4V sample, it drops drastically. This may be due to high stresses developed as a result of excessive deflection occurring in laser-treated TWAS SHS 7170$^{Plus\ B}$ sample. However, this requires further studies to establish the cause of reduced fatigue properties of laser-treated TWAS SHS 7170$^{Plus\ B}$-coated Ti6Al4V sample and its recovery due to proper stress relieving.

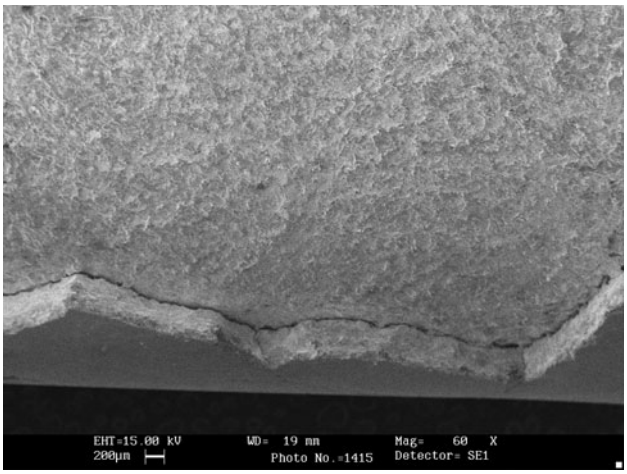

Fig. 13 SEM of laser-treated TWAS SHS 7170 coating at 60× magnification after WDE testing of 47,500 cycles (coating cracked during incubation period in the absence of boride layer)

4. Conclusions

By providing a thin boride bond coat and subsequently treating with HPDL, the bonding of TWAS SHS 7170 coating to Ti6Al4V alloy has improved manifold. Without this layer, it is not possible to bond TWAS SHS 7170 coating to Ti6Al4V alloy. The WDE resistance of this multilayer coating (TWAS SHS 7170$^{Plus\ B}$) has improved significantly compared to

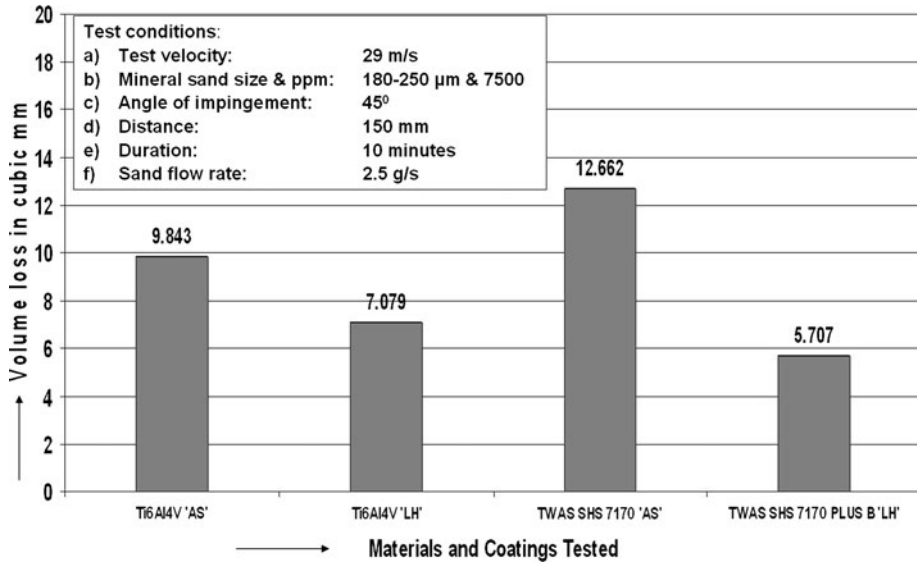

Fig. 14 Volume losses of different materials and coatings due to solid particle erosion

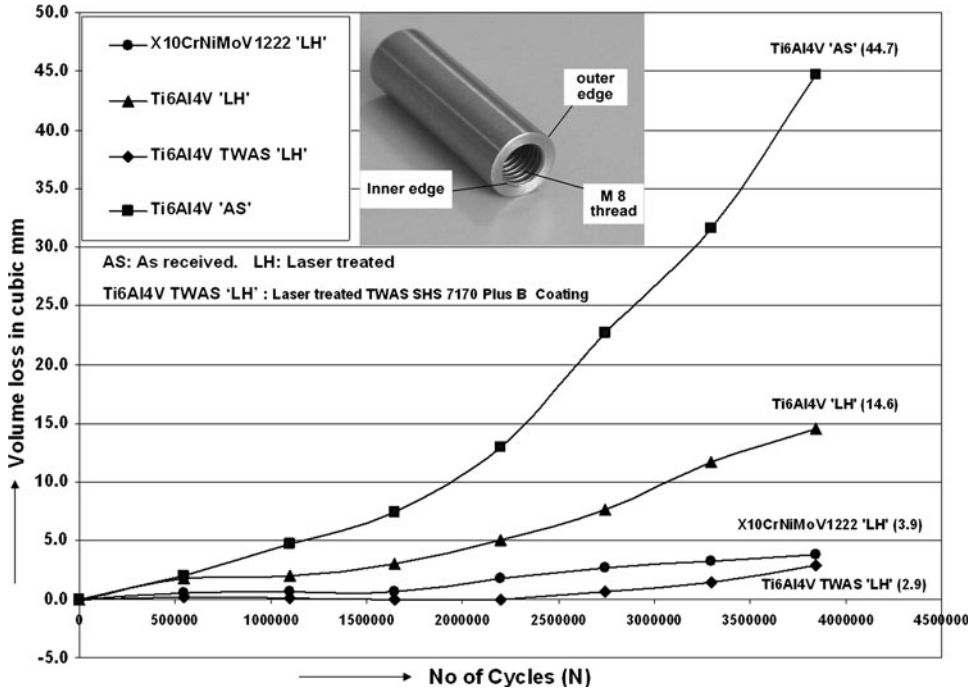

Fig. 15 Volume losses of laser-treated TWAS SHS 7170$^{\text{Plus B}}$ coating and other materials up to 3.84 million cycles at water droplet energy flux of 57.167 million J/m^2 s

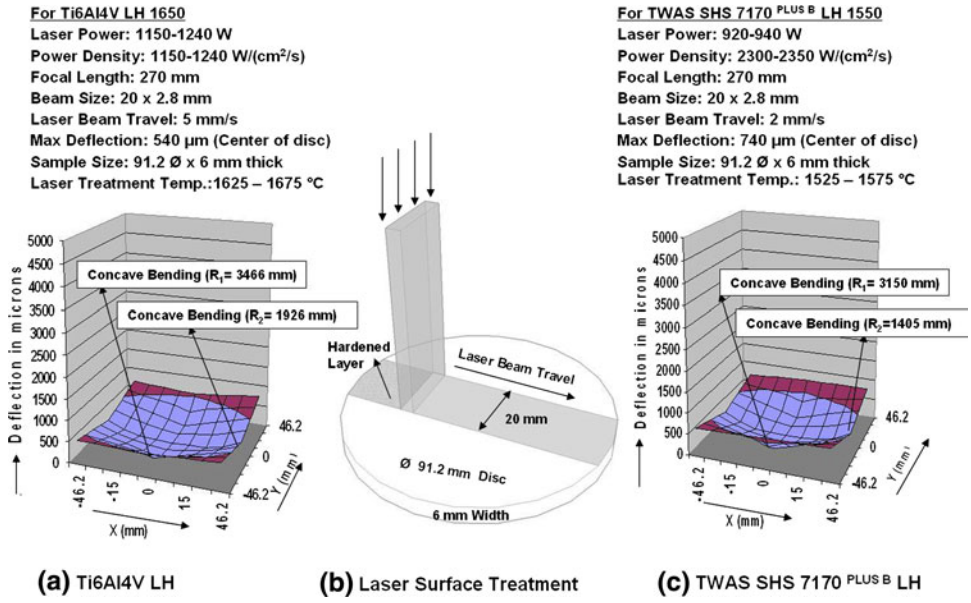

Fig. 16 The affect of laser treatment on the deflection occurring in TWAS SHS 7170$^{\text{Plus B}}$-coated and uncoated Ti6Al4V disc

Table 3 Fatigue test results

Sl. No.	Material tested for reverse bending fatigue	Cycles to failure at a load of 400 MPa	Cycles to failure at a load of 550 MPa
1.	Ti6Al4V AS (as-received)	1,25,000	68,200
2.	Ti6Al4V LH (laser-treated)	1,62,000	58,200
3.	TWAS SHS 7170$^{\text{Plus B}}$ (laser-treated)	22,400	8,400

untreated as well as laser-treated Ti6Al4V alloy. The particulate erosion resistance has also improved approximately two times as compared with "as-sprayed" TWAS SHS $7170^{Plus\ B}$ coating.

The laser-treated TWAS SHS $7170^{Plus\ B}$-coated sample does not show any cracks on applying a load of 30 kg. This coating has developed better adhesion and toughness as compared to the untreated one, and hence gives much better performance in the droplet erosion testing. The "as sprayed" TWAS SHS $7170^{Plus\ B}$ coating has peeled off early during droplet erosion testing (~47,500 cycles) because it has voids, pores, inter boundary defects, and inadequate bonding with the substrate.

The SEM of laser-treated Ti6Al4V alloy sample shows relatively larger grains size as compared to laser-treated TWAS SHS $7170^{Plus\ B}$ coating. The microstructure of laser-treated TWAS SHS $7170^{Plus\ B}$ coating outer layer is free from voids, oxides, and pores and shows the formation of fine needles. This has a direct bearing on grain morphology and has resulted in manifold improvement in WDE resistance.

Due to excellent fracture toughness and adequate micro hardness, the laser-treated TWAS SHS $7170^{Plus\ B}$ coating on Ti6Al4V can be an excellent erosion-resisting shield against foreign objects' damages occurring on the high-rating steam turbine and aero-compressor guide blades. Fatigue properties of laser-treated TWAS SHS $7170^{Plus\ B}$ coating on Ti6Al4V have reduced drastically as compared with untreated Ti6Al4V alloy. Hence, the application of this above coating is limited to stationary components. The fatigue properties of laser-treated Ti6Al4V alloy are comparable to that of untreated Ti6Al4V alloy whereas its droplet erosion resistance is much superior to that of untreated Ti6Al4V alloy. This may be a probable solution for rotating as well as vibrating components where both fatigue and erosion properties are required.

Acknowledgments

The authors are thankful to Mr. Venkateswar Reddy for doing Scanning Electron Microscopy, and Dr. (Mrs.) Y. Kalpana for providing information on water chemistry. The authors are also thankful to the management of Corporate R&D for permission to publish this article.

References

1. E.R. Buchman, *An Overview of Erosion Resistant Coatings for Steam Path Surfaces*, Turbo Machinery International, Jan/Feb 1987, p 25–28
2. B.S. Mann, Solid Particle Erosion and Protective Layer for Steam Turbine Blading, *Wear*, 1999, **224**, p 8–12
3. J.I. Cofer, IV, J.K. Reinker, and W.J. Summer, *Advances in Steam Path Technology*, GE Power Systems Paper, GER-3713
4. W. Tabakoff, M. Metwally, and A. Hamed, High Temperature Coatings for Protection Against Turbine Deterioration, *Trans. ASME J. Eng. Gas Turbine Power*, 1995, **117**, p 146–155
5. M. Metwally, W. Tabakoff, and A. Hamed, Blade Erosion in Automotive Gas Turbine Engine, *Trans. ASME J. Eng. Gas Turbine Power*, 1995, **117**, p 213–219
6. B.S. Mann and V. Arya, HVOF Coating and Surface Treatment for Enhancing Droplet Erosion Resistance for Steam Turbine Blades, *Wear*, 2003, **254**, p 652–667
7. B.K. Pant, V. Arya, and B.S. Mann, Enhanced Droplet Erosion Resistance of Laser-Treated Nano Structured TWAS and Plasma Ion-Nitro Carburized Coatings for High-Rating Steam Turbine Components, *J. Therm. Spray Tech*., Published online 30th April, 2010
8. D.J. Brangan, M. Breitsameter, B.E. Meacham, and V. Belashchenko, High Performance Nano Scale Composite Coating for Boiler Applications, *J. Therm. Spray Tech.*, 2005, **14**(2), p 196–204
9. B.Q. Wang and M.W. Seitz, Comparison in Behavior of Iron Base Coatings Sprayed by Three Different Arc Spray Processes, *Wear*, 2001, **250**, p 755–761
10. S. Dallaire, Hard Arc-Sprayed Coatings with Enhanced Erosion and Abrasion Wear Resistance, *J. Therm. Spray Tech.*, 2001, **10**(3), p 511–519
11. S. Dallaire, H. Levert, and J.G. Legoux, Erosion Resistance of Arc-Sprayed Coatings to Iron Core at 25 and 315 °C, *J. Therm. Spray Tech.*, 2001, **10**(2), p 337–350
12. P. Georgieva, R. Thorpe, A. Yanski, and S. Seal, Nano Composite Materials, an Innovative Turnover for the Wire Arc Spraying Technology, *Adv. Mater. Process.*, 2006, **164**(8), p 68–69
13. Industrial News, New Benchmark Achieved with the Development of Nanoscale coatings Using Electric Arc Spraying, *J. Therm. Spray Tech*., 2005, **14**(1), p 13
14. S. DePalo, M. Mohanty, H. Marc-Charles, and M. Dorfman, Fracture Toughness of HVOF Sprayed WC-Co Coatings, *Therm. Spray: Surf. Eng. Appl.*, 2000, **5**, p 245–250
15. V. Gorokhovsky, C. Bowman, J. Wallace, D. Van Vorous, J. O'Keefe, V. Champagne, M. Pepi, and W. Tabakoff, LAFAD Hard Ceramic and Cermet Coatings for Erosion and Corrosion Protection of Turbo Machinery Components, *Proceedings of ASME Turbo Expo 2009: Power for Land, Sea and Air*, GT 2009-59391, 8-12 June 2009, Orlando, Florida, USA, p 1–38
16. J.R. Cheski, R. Patel, K. Rockaway, H. Osaghae, and M. Christianson, A Large Steam Turbine Retrofit Design and Operation History, *Presented at 2005 Power-Gen International Conference Held at Las Vegas, NV*, 6 Dec 2005
17. A. Mujezinovic, Bigger Blades Cut Costs, *Modern Power Syst*., 2003, **23**(2), p 25–27
18. B. Stanisa and V. Ivnsic, Erosion Behavior and Mechanism for Steam Turbine Rotor Blades, *Wear*, 1995, **186–187**, p 395–400
19. B. Stanisa, Z. Schauperl, and K. Grilec, Erosion Behavior of Turbine Rotor Blades Installed in the Krsko Nuclear Power Plant, *Wear*, 2003, **254**, p 735–741
20. B.S. Mann, V. Arya, and P. Joshi, Advanced HVOF Coating and Candidate Materials for Protecting LP Steam Turbine Blades Against Droplet Erosion, *J. Mater. Eng. Perform.*, 2005, **14**(4), p 487–494
21. M. Naeem, Heat Treating with Lasers, *Heat Treating Prog*., 2005, **5**(3), p 47–51
22. C. Phipps, Laser Applications Overview, The State of Art and the Future Trend in United States, *RIKEN Rev.* 2003, **50**, p 11–19, Focused on Laser Precesion Microfabrication (LPM 2002)
23. B.S. Mann, V. Arya, A.K. Maiti, M.U.B. Rao, and P. Joshi, Corrosion and Erosion Performance of HVOF/TiAlN PVD Coatings and Candidate Materials for High Pressure Gate Valve Application, *Wear*, 2006, **260**, p 75–82
24. B.S. Mann, V. Arya, B.K. Pant, and M. Agrawal, High-Power Diode Laser Surface Treatment to Minimize Droplet Erosion of Low-Pressure Steam Turbine Moving Blades, *J. Mater. Eng. Perform.*, 2009, **18**(7), p 990–998